Phase Behavior of Columnar DNA Assemblies

H. M. Harreis,[1] A. A. Kornyshev,[1,2,3] C. N. Likos,[1] H. Löwen,[1] and G. Sutmann[4]

[1]*Institut für Theoretische Physik II, Heinrich-Heine-Universität Düsseldorf, Universitätsstraße 1, D-40225 Düsseldorf, Germany*
[2]*Research Centre Jülich, D-52425 Jülich, Germany*
[3]*Department of Chemistry, Imperial College, London SW7 2AY, United Kingdom*
[4]*John von Neumann Institute for Computing, Research Centre Jülich, D-52425 Jülich, Germany*

(Received 4 December 2001; published 17 June 2002)

The interaction between two stiff parallel DNA molecules depends not only on the distance between their axes but also on their azimuthal orientation. The positional and orientational order in columnar *B*-DNA assemblies in solution is investigated, on the basis of the electrostatic pair potential that takes into account DNA helical symmetry and the amount and distribution of adsorbed counterions. A phase diagram obtained by lattice sums predicts a variety of positionally and azimuthally ordered phases and bundling transitions strongly depending on the counterion adsorption patterns.

DOI: 10.1103/PhysRevLett.89.018303 PACS numbers: 82.35.Rs, 64.70.–p, 82.70.Dd, 87.14.Gg

DNA is a polyelectrolyte molecule and it disassociates in aqueous solution: Its cations go into solution, leaving behind negative charges on the phosphates of the DNA backbone. A considerable fraction of the cations condenses in a Bjerrum layer around the molecular surface [1], but if there are ions in the solution that specifically adsorb onto DNA, its surface could be almost fully neutralized [2] or even overcharged [3]. Far from their axes, DNA molecules can be apprehended as charged cylinders. If charges were smeared continuously along the cylinders, two such molecules would repel each other electrostatically (with the repulsion exponentially screened by the electrolyte). However, the net charge distribution on the molecules is not homogeneous and this changes dramatically the interaction potential at intermediate distances. Indeed, in order to condense DNA in an aggregate, one has either to apply osmotic stress [4] or use condensing agents, such as salts with Mn^{2+}, Cd^{2+}, spermidin, protamine, or cobalt hexammine [5] cations. These cations are known to specifically adsorb on DNA, predominantly into the DNA *grooves* [6]. Other counterions, such as, e.g., Ca^{2+} or Mg^{2+}, that have strong affinity to phosphates and adsorb preferentially on the *strands* do not induce DNA aggregation. The adsorbing counterions reduce the net charge on the DNA. Had that been their only effect, it would have been hard to explain the sensitivity of DNA aggregation [5] and of the mesomorphism of the resulting aggregates [7] to the sort of counterions.

Recently, a new explanation of the features of DNA aggregation was suggested [8], resting on a Debye-Bjerrum theory of electrostatic interaction between parallel helical macromolecules, such as, e.g., double stranded B and A forms of DNA [9,10]. Various patterns of adsorbed counterions, including those spiraling through DNA major and minor grooves, were considered. Thus, the effect of helically structured separation between negative and positive charges on each molecule was rationalized, explaining, e.g., a stronger DNA-DNA attraction in the presence of the counterions that adsorb preferentially into the major groove. Consequences of the theory [10] proved to be in line with experiments. The properties of the calculated interaction potential were verified by computer simulations [11].

A remarkable effect of DNA double strandedness is a peculiar dependence of the interaction potential $u(R, \phi)$ on the mutual azimuthal orientation angle, ϕ (see Fig. 1) [9]: $u(R, \phi) \cong C(R) - A(R)\cos\phi + B(R)\cos^2\phi$, where $A(R)$, $B(R), C(R) > 0$ depend on the parameters of DNA structure and distribution of adsorbed ions, and $A(R) > B(R)$ at large interaxial separations R. This potential has two symmetric azimuthal minima at $\hat{\phi}_{\pm} \neq 0$ for distances smaller than a critical one at which $A(R) = 2B(R)$, and one minimum at $\hat{\phi} = 0$ for larger R. Thus the problem of statistical properties of columnar aggregates of long rigid DNA molecules [13] can be mapped on a 2D problem of XY spins interacting via this unusual potential with dominant nearest neighbor interactions, as $A(R)$ and $B(R)$ exponentially decrease with R. While the $\hat{\phi} = 0$ case is compatible with a hexagonal lattice, $\hat{\phi} \neq 0$ results in frustrations of positional and orientational order [14]. Because of the "$R - \phi$ coupling" in the interaction potential, one may expect peculiar positional and "spin" structures in the aggregate, a feature known as the mesomorphism of DNA assemblies [7].

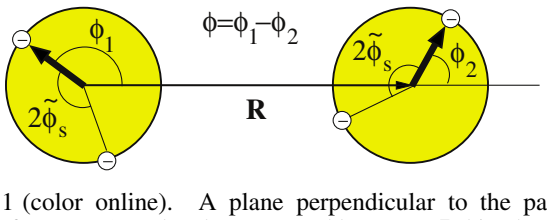

FIG. 1 (color online). A plane perpendicular to the parallel axes of two DNA molecules separated by vector **R** hits the DNA strands denoted by the white circles; $2\tilde{\phi}_s$ is the azimuthal width of the minor groove. The vectors joining the axes with the points where the $5' - 3'$ strand [12] hits the plane may be formally called "spins." The angle ϕ between the two spins characterizes mutual azimuthal orientation of the molecules.

In this work, we analyze the statistical properties of such assemblies in aqueous solutions. We calculate the *ground state* phase diagrams [15] that depend on the DNA and salt concentrations, and on the counterion adsorption pattern. To investigate the stability of various phases, we calculate lattice sums for interacting DNA molecules and supplement them with the entropic and cohesive contributions from the ions of the solution. The so-obtained variational Helmholtz free energy is finally minimized among the candidate phases.

To model the interaction, we envision the molecules as long cylinders, carrying helical, continuous line charges on their surfaces. Each DNA duplex carries the negative charge of phosphates with surface charge density $\sigma = 16.8\ \mu\mathrm{C/cm}^2$ plus a compensating positive charge coming from the adsorbed counterions. Let $0 < \theta < 1$ be the degree of charge compensation, f_1, f_2, and f_3 the fractions of condensed counterions in the minor and major grooves, and on the two strands, respectively ($f_1 + f_2 + f_3 = 1$). The mobile counterions in solution screen the Coulomb interactions between the helices, causing at large separations an exponential decay of the latter with the Debye screening length κ^{-1}. The solvent is accounted for by its dielectric constant ε. The structural parameters of B-DNA are $\tilde{\phi}_s \approx 0.4\pi$, pitch $H \approx 34$ Å ($g = 2\pi/H$), and hard-core radius $a = 9$ Å. For the pair interaction potential, we take the following form [8] ($R > 2a$):

$$\frac{u(R,\phi)}{u_0} = \sum_{n=-\infty}^{\infty} [f_1\theta + (-1)^n f_2\theta - (1 - f_3\theta)\cos(n\tilde{\phi}_s)]^2 \frac{(-1)^n \cos(ng\Delta z) K_0(\kappa_n R) - \Omega_{n,n}(\kappa_n R, \kappa_n a)}{(\kappa_n/\kappa)^2 [K_n'(\kappa_n a)]^2}, \quad (1)$$

where Δz is a vertical displacement, equivalent to a "spin angle" $\phi = g\Delta z$. Here, $u_0 = 8\pi\sigma^2/\varepsilon\kappa^2$ ($\approx 2.9 k_B T/$Å at physiological ionic strength), and $\kappa_n = \sqrt{\kappa^2 + n^2 g^2}$. $\Omega_{n,m}(x,y)$ is given by

$$\Omega_{n,m}(x,y) = \sum_{j=-\infty}^{\infty} \left[K_{n-j}(x) K_{j-m}(y) \frac{I_j'(y)}{K_j'(y)} \right], \quad (2)$$

with the modified Bessel functions $K_n(x)$ and $I_j(y)$. The primes denote derivatives. The ϕ dependence is affected by the distributions f_i, $i = 1,2,3$ of the condensed counterions [8]. Keeping only the $n = 0$ term in the sum of Eq. (1) returns a pair potential of homogeneously charged cylinders, depending on R only. The approximation $u(R,\phi) \cong C(R) - A(R)\cos\phi + B(R)\cos^2\phi$ results from truncating the sum at $|n| = 2$. Because of rapid convergence of the sum, truncation at $|n| = 5$ suffices.

For all cases studied in this work, the pair potential is greater than $k_B T$, thus we focus on the ground state analysis of the basic structures of the assembly. To this end, we considered the five two-dimensional Bravais lattices, i.e., the hexagonal (HEX), square (SQ), rectangular (REC), rhombic (RHO), and oblique (OBL) lattices. In order to explore the *ordered* spin structures, we constructed a certain spin pattern on the elementary plaquette of every lattice and repeated it along the lattice directions. Without spin-spin interactions beyond the elementary plaquette of the lattice, the exact ground state can be obtained as follows. The energy of the plaquette must be minimized with respect to the spin angles, and the optimized spin pattern of the plaquette repeated throughout the lattice. We have kept interactions of higher-order neighbors but the nearest-neighbor interactions dominate due to the exponential decay of the R-dependent prefactors.

In Fig. 2 we show schematically the algorithms employed for the generation of the ordered spin structures. Choosing the orientation of one of the spins as reference ($\phi = 0$), we are left with two free orientations per plaquette for the HEX lattice and three for the REC and SQ lattices. The lattice is filled by successive mirror reflections of the cells across their edges, as shown in Figs. 2(a) and 2(b). As far as the RHO and OBL lattices are concerned, the procedure involving three free spin angles per plaquette does not generate identical plaquettes upon reflection: For these lattices, there is a short and a long diagonal which exchange their roles upon reflection. We employ two complementary algorithms for generating ordered magnetic structures on these lattices: First, we place spins of orientations ϕ_1 and ϕ_2 along the cell edges and $\phi_1 - \phi_2$ along the long diagonal and use the successive reflection algorithm. This guarantees that all pairs of spins across all diagonals will have relative angles $\phi_1 - \phi_2$ [see Fig. 2(c)]. Alternatively, we place along the long diagonal a spin with an angle $\phi_1 + \phi_2$ and, subsequently, we increase the spin angle along the horizontal direction by an amount of ϕ_1, and along the oblique direction by an amount of ϕ_2 for every step. We thus generate structures in which all spins along the short diagonals have an angle $\phi_2 - \phi_1$ and all spins along the long diagonals an angle $\phi_1 + \phi_2$, as shown in Fig. 2(d).

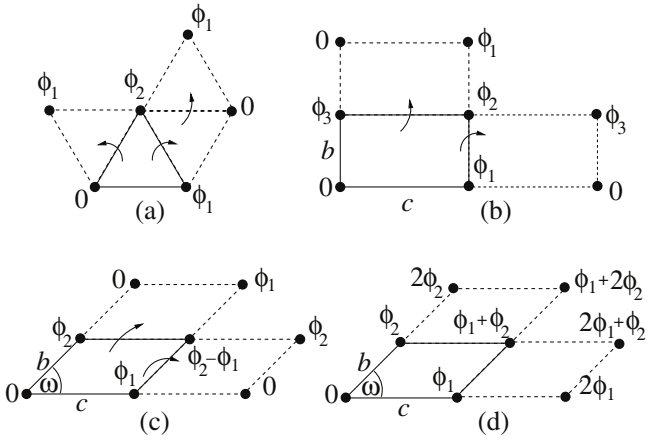

FIG. 2. A schematic view of generating candidate ordered spin phases of the system. (a) For the HEX lattice; (b) for the REC and SQ lattices; (c),(d) for the RHO and OBL lattices.

Using Eq. (1), the interaction between two stiff molecules is $L_p u(R, \phi)$, with the persistence length $L_p = 500$ Å. It was found that the energy needed to destroy the translational or orientational order must be more than several $k_B T$ at room temperature; hence, the lattice-sum calculations provide the representative thermodynamic states. The 2D DNA concentration ρ was varied within $0 \leq \rho a^2 \leq 1/(2\sqrt{3})$, the upper limit being the close-packed configuration in a HEX lattice [16]. For every density, minimizations of the lattice energy were carried out, with respect to the plaquette sets $\{\phi_i\}$, the size ratios b/c (for the REC lattice), and/or the geometrical angle ω (RHO and OBL lattices) (Fig. 2). The optimized lattice-sum energy, $U_X(\mathbf{\Phi}, \rho)$, was obtained, where X stands for the lattice type and $\mathbf{\Phi} = (\phi_1, \phi_2, \ldots, \phi_N)$ denotes the configuration of the N spins in the system. The low-density 2D fluid was taken into account as follows: For every κ, the pair potential of Eq. (1) for $\phi = 0$ was mapped onto an effective hard-disk one, by means of the Barker-Henderson rule [17]. Using the effective hard-disk diameter $d(\kappa)$ and the known result $(\pi/4)\rho_m d^2 = 0.691$ for the melting density of hard-disk systems [18], the melting line was estimated [see Fig. 4(a) (below)].

To access the full thermodynamics of the DNA solution-salt mixture, we have to add the contributions to the free energy from the counter- and co-ions (numbers $N_\pm$ and concentrations $c_\pm$, respectively). These degrees of freedom contribute an extensive term to the free energy of the system [19], $F_c = F_+^0 + F_-^0 + F_{coh}$, where $F_\pm^0 = N_\pm k_B T[\ln(c_\pm \Lambda_\pm^3) - 1]$ are the ideal-gas contributions (where $\Lambda_\pm$ are the thermal de Broglie wavelengths of the counter- and co-ions) and

$$F_{coh} = -\frac{1}{2}\left[\frac{2Na(Ze)^2\kappa}{\varepsilon L_p(1 + \kappa a)} + \frac{k_B T V(c_+ - c_-)^2}{c_+ + c_-}\right], \tag{3}$$

is a cohesive term. In Eq. (3), e is the electron charge, $Z|e| = 2\pi a L_p \sigma(1 - \theta)$ is the uncompensated DNA charge, $c_+ = Z\rho/L_p + n_s$ and $c_- = n_s$, with the salt concentration n_s. Finally, V is the volume of the system and $\kappa = \sqrt{4\pi(Z\rho/L_p + 2n_s)e^2/(\varepsilon k_B T)}$ for monovalent salt ions. The Helmholtz free energy is $U_X + F_c$.

When counterions are condensed *on strands,* i.e., $f_1 = f_2 = 0$ and $f_3 = 1$, the DNA-DNA interaction is purely repulsive. The system is found to crystallize into the HEX lattice at all DNA densities but a large variety of orientational (magnetic) structures occurs, as a result of the frustration of the system. The structures are shown in Fig. 3 and the phase diagram of the DNA-salt mixture in Fig. 4(a). The FM phase is ferromagnetic: All DNA molecules have the same azimuthal orientation. The phase denoted AFI displays antiferromagnetic-Ising ordering, with half of the DNA molecules having one azimuthal orientation on one of the sublattices and a different on the other. The AFP phase has a three-state antiferromagnetic Potts [20] type of ordering, with 1/3 of the spins pointing in a reference direction $\phi = 0$, 1/3 in the angle ϕ_0, and 1/3 in the angle $2\phi_0$, where ϕ_0 grows with DNA concentration. Finally, the AFH phase has the orientational ordering of the two-dimensional antiferromagnetic Heisenberg model, with spins residing in the three sublattices of the hexagonal lattice having mutual orientational angles of 120° to one another. The transition between the FM and the AFP phases is second order, but the AFP → AFI and AFI → AFH transitions are first order with very narrow density gaps [21]. The FM phase is stable at low DNA concentrations [see Fig. 4(a)]. For such average intermolecular separations, the optimal azimuthal angle between the molecules is zero. The nontrivial phases arise at higher densities of the aggregates, as a result of the frustrated character of the ϕ dependence of the pair potential. Similar mesophases were found recently within the framework of a phenomenological Landau theory [23].

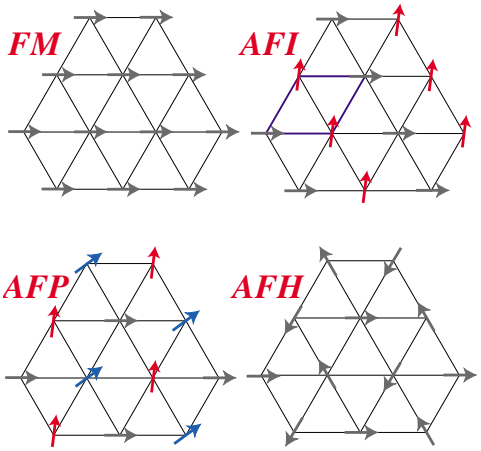

FIG. 3 (color online). The four stable "magnetic" phases. The arrows indicate the azimuthal orientations of DNA molecules. The acronyms, using magnetic terminology, stand for *ferromagnetic* (FM), *antiferromagnetic Ising* (AFI), *antiferromagnetic Potts* (AFP), and *antiferromagnetic Heisenberg* (AFH).

When counterions condense *in grooves,* an attraction between the DNA molecules arises, since the positively charged sections of one molecule can approach the negatively charged sections of the other through an appropriate mutual orientation [8]. This leads to broad phase-coexistence lines between dense DNA aggregates and DNA-free solutions. This is demonstrated in Fig. 4(b) for the case $f_1 = 0.3$, $f_2 = 0.7$, and $f_3 = 0$ for $\theta = 0.7$. Increasing θ to 0.9 results in DNA-aggregate coexistence with DNA-free solutions at all salt concentrations [see Fig. 4(c)]. The oblique tielines result from the requirement that the electrolyte chemical potentials be equal at both coexisting phases. In the one-phase region, a rhombic phase shows up for moderate to high densities and a HEX crystal appears at very high DNA concentrations. A strong *qualitative* difference in the macroscopic behavior of columnar DNA assemblies arises, depending on whether the counterions condense on strands or in

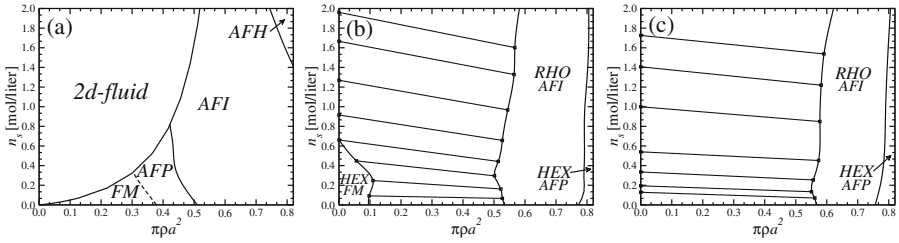

FIG. 4. Phase diagrams of DNA-salt mixtures: (a) $\theta = 0.9$, $f_3 = 1$; the lattice here is HEX. (b) $\theta = 0.7$, $f_1 = 0.3$, $f_2 = 0.7$; (c) $\theta = 0.9$, $f_1 = 0.3$, $f_2 = 0.7$. Dashed lines denote second-order magnetic transitions, solid lines first-order ones. The geometrical transitions between different lattices in (b) and (c) are second order; the straight lines are tielines between coexisting phases. The phase diagrams are plotted as a function of the electrolyte concentration in the aggregate. Taking into account the Donnan equilibrium [22], the diagrams, recalculated as a function of the salt in the reservoir, are qualitatively the same as the ones shown.

grooves. In the former case, all transitions are in the azimuthal variables. In the latter, DNA bundling in rhombic structures takes place. Holding $f_1 = 0.3$ and increasing f_2 at the cost of f_3, the crossover to bundling topology occurs, e.g., for $\theta = 0.7$ at $(f_2, f_3) = (0.63, 0.07)$.

The predictions of the theory ask for experimental verification. Such a task is not easy, since the reliable data until now refer only to highly concentrated phases [24], where the number of the basic assumptions inherent to the form of the pair potential may be questioned (the Debye-Bjerrum approximation, independence of solvent dielectric constant on the aggregate density, effects of nonlocal polarizabilty, etc.). The increase of experimental resolution in x-ray diffraction could open the way for the study of less dense aggregates. The predicted specific effect of cation adsorption on the phase diagram is particularly challenging. Since the adsorption isotherms and the distributions of the adsorbed ions are poorly known, one should concentrate here on qualitative effects, i.e., the (dis)appearance of mesophases triggered by different DNA condensing counterions.

We thank A. Cherstvy, A. Esztermann, S. Leikin, and A. Parsegian for useful discussions and acknowledge support by the DFG, Grants No. LO 418/6 and No. KO 139/4.

[1] G. S. Manning, Q. Rev. Biophys. **11**, 179 (1978).
[2] R. W. Wilson and V. A. Bloomfield, Biochem. **18**, 2192 (1979); J. Widom and R. L. Baldwin, J. Mol. Biol. **144**, 431 (1980); P. G. Heath and J. M. Schurr, Macromolecules **25**, 4149 (1992).
[3] J. Pelta, F. Livolant, and J.-L. Sikorav, J. Biol. Chem. **271**, 5656 (1996).
[4] D. C. Rau, B. Lee, and V. A. Parsegian, Proc. Natl. Acad. Sci. U.S.A. **81**, 2621 (1984).
[5] V. A. Bloomfield, Curr. Opin. Struct. Biol. **6**, 334 (1996).
[6] A. H. A. Tajmir-Riahi *et al.,* J. Biomol. Struc. Dyn. **11**, 83 (1993); I. Fita *et al.,* J. Mol. Biol. **167**, 157 (1983); N. V. Hud *et al.,* Biochem. **33**, 7528 (1994); X. Shui *et al.,* Biochem. **37**, 8341 (1998).
[7] R. Podgornik, H. H. Strey, and V. A. Parsegian, Curr. Opin. Colloid Interface Sci. **3**, 534 (1984).
[8] A. A. Kornyshev and S. Leikin, Phys. Rev. Lett. **82**, 4138 (1999).
[9] A. A. Kornyshev and S. Leikin, J. Chem. Phys. **107**, 3656 (1997); **108**, 7035(E) (1998).
[10] A. A. Kornyshev and S. Leikin, Proc. Natl. Acad. Sci. U.S.A. **95**, 13 597 (1998); Biophys. J. **75**, 2513 (1998); Phys. Rev. Lett. **86**, 3666 (2001).
[11] E. Allahyarov and H. Löwen, Phys. Rev. E **62**, 5542 (2000).
[12] R. R. Sinden, *DNA Structure and Function* (Academic, New York, 1994).
[13] Treating DNA molecules as rigid is justified as long as their contour length does not exceed the persistence length $L_p = 500$ Å.
[14] H. H. Strey *et al.,* Phys. Rev. Lett. **84**, 3105 (2000).
[15] This is meaningful as far as the interaction energy exceeds $k_B T$, which is true for long DNA fragments within the density range of DNA columnar phases.
[16] The molecules remain parallel down to density $\rho a^2 \approx 0.1$, corresponding to interaxial separations $R \approx 34$ Å, at which the cholesteric phase (CP) appears [F. Livolant, Physica (Amsterdam) **176A**, 117 (1991)]. A theory of the CP is beyond the scope of this Letter, thus we draw our phase diagrams down to $\rho a^2 = 0$, with the reminder that for large interaxial separations the CP is stable.
[17] J.-P. Hansen and I. R. McDonald, *Theory of Simple Liquids* (Academic, London, 1986), 2nd ed.
[18] A. C. Mitus, H. Weber, and D. Marx, Phys. Rev. E **55**, 6855 (1997).
[19] H. Graf and H. Löwen, Phys. Rev. E **59**, 1932 (1999).
[20] J. M. Yeomans, *Statistical Mechanics of Phase Transitions* (Clarendon, Oxford, 1992).
[21] H. Graf and H. Löwen, Phys. Rev. E **57**, 5744 (1998).
[22] S. A. Rice, M. Nasagawa, and H. Morawetz, *Polyelectrolyte Solutions* (Academic, New York, 1961).
[23] V. Lorman, R. Podgornik, and B. Žekš, Phys. Rev. Lett. **87**, 218101 (2001).
[24] R. Langridge *et al.,* J. Mol. Biol. **2**, 19 (1960); S. D. Dover, J. Mol. Biol. **110**, 699 (1977); H. Grimm and A. Ruprecht, Physica (Amsterdam) **174B**, 291 (1991).